Polymer Solutions, Blends, and Interfaces
I. Noda and D.N. Rubingh (editors)

The Influence of the Fiber/Matrix Interface on Local Glass Transition Temperature

N.R. Sottos

Department of Theoretical and Applied Mechanics
University of Illinois at Urbana-Champaign
Urbana, IL 61801

Abstract

Determining the local structure and properties of the interphase is crucial to understanding how the interphase influences overall thermo-mechanical behavior of a composite. Several theoretical investigations have presented evidence for the existence of an interphase region with a glass transition temperature that is significantly lower than that of the neat resin. In the current study both interferometric measurements and single fiber critical length tests are performed on samples with tailored interphases to further investigate variations in local glass transition temperature and its influence on micro-mechanical behavior. Two different interphase conditions are considered: fibers coated with a low T_g resin and untreated fibers (no coating). Micro-interferometry was utilized to study differences in thermally induced axial displacements for the two different interphase conditions. Additionally, single fiber critical length tests were performed over a range of temperatures to determine the effects of the interphase glass transition on the value of interfacial shear strength. Experimental results support the existence of a reduced glass transition temperature near the fiber surface.

1. INTRODUCTION

Although the exact physical and chemical mechanisms are not clearly understood, it is widely believed that an interphase region with properties that differ from those of the neat matrix is developed near fiber surfaces in polymer matrix composites. In thermosetting systems, the interphase may result from changes in the cure chemistry of the resin near the fiber surface. Early on, Erickson et al. [1] proposed that the surface properties of glass fibers could cause some of the constituents in a thermosetting matrix to be adsorbed, deactivated or destroyed. An enrichment of the amine curing agent was shown to develop near the fiber surface. Lipatov, et al. [2] demonstrated that fillers effect the relaxation time spectra of filled polymer systems. It was proposed that the presence

of the filler restricted the molecular mobility of the epoxy matrix. Papanicolaou, et al. [3] used differential scanning calorimetry to measure changes in heat capacity with temperature for both a filled and unfilled epoxy system. Estimates of an interphase volume fraction were based on differences in the jumps of the heat capacity of the two systems in the glass transition region. Using infrared attenuated internal reflectance (IR) spectroscopy, Garton and Daly[4] showed that simulated reinforcement surfaces of both carbon and aramid modify the crosslinking chemistry in the epoxy matrix next to the surface.

More recently, Palmese[5] has shown that the presence of carbon fibers can alter the reaction behavior in thermosetting systems. Palmese performed extensive studies of the diffusion related structural modifications of a Shell EPON 828/PACM 20 epoxy matrix. For this particular system, a stoichiometric imbalance of epoxy resin and amine curing agent developed near graphite fiber surfaces. The cross-link density, epoxy concentration and amine concentration were predicted as a function of radial distance from the fiber surface. Gradients in the amine concentration are likely to create gradients in material properties such as elastic modulus, coefficient of thermal expansion, and the glass transition temperature, T_g . In particular, evidence of an interphase with a reduced glass transition temperature has appeared in the literature and is summarized in the next section.

In the current investigation, the influence of interphase glass transition temperature on thermo-mechanical behavior was investigated for single carbon fiber/epoxy matrix composites. Two different interphase conditions were considered. In the first condition, carbon fibers were coated with a low T_g resin, while for the second the fibers were left untreated (no coating). Micro-interferometry was utilized to study differences in thermal displacements for the two different interphase conditions (see Section 3.2). Through a comparison of the experimental profiles with theoretical predictions, trends in interphase material properties were assessed. Additionally, single fiber critical length tests were performed over a range of temperatures for samples with the two different interphase conditions. The effects of the interphase glass transition on the value of interfacial shear strength was investigated.

2. EVIDENCE OF A REDUCED LOCAL GLASS TRANSITION

Several researchers have found evidence of an altered local glass transition temperature in composite materials. For example, Pogany [6] first showed that non-stoichometric concentrations of an aliphatic polyamine crosslinked with an epoxy resin can lead to reductions in the glass transition temperature. Lipatov, et al. [2] concluded a selective sorption of one of the components in a filled epoxy system may occur on the filler surface before hardening. A surplus of the other component may act as a plasticizer which causes a reduction of elastic moduli and a change in the relaxation behavior of the filled system. Crowson and Arridge [7] observed a difference in glass transition temperature between filled and unfilled epoxy systems. Additionally, Papanicolaou, et al. [8] discussed the

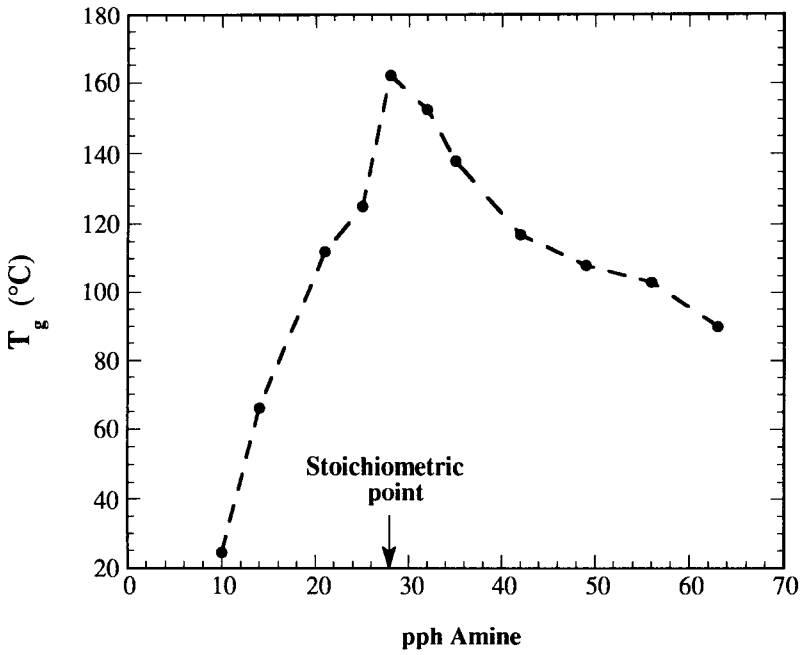

Figure 1: Variation of glass transition temperature with amine concentration.

existence of a viscoelastic interphase with a lower glass transition temperature .

Palmese [5] has measured changes in glass transition temperature as a function amine concentration for the EPON 828/PACM 20 system using both dynamic and thermal mechanical analysis (DMA and TMA). The results are presented in Figure 1. The width of the transition at each concentration is fairly narrow (approximately $30°C$). At the stoichiometric point (28 parts PACM 20 to 100 parts EPON 828), the glass transition temperature is $160°C$. For amine concentrations both above and below the stoichiometric point, the value of T_g is significantly reduced. If the fiber surface alters the cure chemistry such that a non-stoichometric mixture of amine and epoxy occurs, the material in that region would in theory have a much lower glass transition temperature than the neat resin.

Recent investigations by Sottos, et al. [16] have presented in-situ experimental evidence for the existence of an interphase region with a glass transition temperature that is significantly lower than that of the neat resin. Thermal displacements were measured using a scanning micro-interferometer for samples consisting of a single carbon fiber embedded in an epoxy matrix. The fibers used for the study were untreated 30 μm pitch base carbon fibers. To heat the sample, a small current was passed through the fiber. As a result, the temperature in the fiber was nearly constant at $70°C$, while the matrix

temperature decreased logarithmically away from the interface.

Comparison of experimental profiles measured by the interferometer with theoretical displacement predictions indicated that the value of the matrix properties near the fiber surface differed appreciably from their value in the neat resin. The difference between the experimental and theoretical curves when no interphase was considered was too large to be accounted for by experimental error or small variations in the properties of the matrix. A thin interphase region of approximately 0.06 fiber radii, with a modulus an order of magnitude lower than the neat resin, most closely matched the experimental profiles. In order for the modulus to be this low, the epoxy in this region would have to be heated to a temperature above its glass transition. Hence, it was proposed that heating to $70°C$ during the experiment caused the material in a thin interphase to exceed its glass transition temperature. The surrounding matrix, sufficiently far from the fiber, was unaffected by this phenomenon.

The existence of a reduced glass transition temperature has significant implications for the thermal behavior and long term performance of a composite. If the interphase had a lower glass transition temperature, the region would have a pronounced effect on the fracture toughness, durability and local stress state of the composite. Such a low modulus region would act to arrest crack growth in the matrix and significantly increase the fracture toughness. On the other hand, the performance of the composite would be significantly reduced at high temperatures. Consequently, the interphase has the potential to be tailored to enhance or hinder these effects depending on the application.

In the current investigation, the interphase was tailored to enhance the effects of a low glass transition temperature. Interferometric measurements were made on samples consisting of a single 30 μm carbon fiber coated with a low T_g resin and embedded in an epoxy matrix. Additionally, single fiber critical length tests were were performed over a range of temperatures for samples consisting of 7 μm AS4 carbon fibers coated with the same low T_g resin.

3. MICRO-INTERFEROMETRIC MEASUREMENTS

Micro-interferometry was utilized to study differences in the thermal displacements caused by changing the interphase glass transition temperature. As mentioned in Section 2, there is evidence the interphase region associated with untreated fibers (no coating) has a lower glass transition temperature than the neat resin. Hence, the thermal displacement behavior observed for untreated fibers should be enhanced by coating the fibers with a low T_g resin.

The interferometric technique for measuring thermal displacements essentially evolved from studies by Scott, et al.[10,11] and Huber, et al.[12] which described a technique for measurement of sub-micron displacements caused by ultrasonic waves propagating at frequencies of one megahertz and above. A distinguishing feature of these earlier methods was the formation of a magnified image on the face of a scanning detector, while the sample served as a stationary mirror in one arm of the interferometer. By using a

scanning detector window with a diameter smaller than the obtainable resolution of the image, detailed displacement contour plots were made without the necessity for continuous realignment of the specimen. From these preliminary designs, a micro-interferometric technique was developed with the capability of measuring thermal displacements with an out-of-plane resolution of 50 angstroms and a possible in-plane resolution of 0.5 μm.

A detailed description of the interferometric experimental technique utilized for the current measurements is given by Sottos, et al.[9,13] and Ryan, et al. [14]. A single, linearly polarized light beam from an Argon laser is incident upon a 40 MHz acousto-optic modulator (AOM) producing two beams which are sent along different arms of the interferometer. The first beam (reference beam) propagates with the same frequency as the beam incident upon the AOM. The second beam is shifted in frequency by 40 MHz and is used to illuminate the sample surface. The two beams are recombined in a beam splitter and then arrive at the primary lens of a long distance microscope. An image is formed behind the microscope and is magnified onto the image plane of a scanning photodiode detector using an eyepiece lens. The light that forms the sample image differs in frequency by 40 MHz from the light that forms the reference image. Thus, any z-axis displacement of the sample surface will produce phase shifts in the 40 MHz beat signal arriving at the photodetector. A lock-in amplifier is used to compare the phase of the 40 MHz signals from both the reference and the scanning detectors.

3.1 Sample Preparation

Thermal displacement measurements were made on specimens consisting of a single carbon fiber embedded in epoxy. A schematic of a specimen is shown in figure 2. The fibers used for this study were untreated 30 μm pitch base carbon fibers supplied by Textron. The properties of these fibers are listed in table 1. The value for Young's modulus, E, was specified by the manufacturer, while the values for the longitudinal thermal expansion coefficient, α, thermal conductivity, K, and Poisson's ratio, ν, were taken from the literature [15]. Shell EPON Resin 828 (diglycidyl ether of bisphenol A*) cured with AMICURE PACM [bis (p-aminocyclohexyl) methane] was chosen as the matrix material. Properties of the neat resin are also given in table 1. The modulus, Poisson's ratio and thermal conductivity were obtained from the manufacturer, while the coefficient of thermal expansion was determined from Thermal Mechanical Analysis (TMA) [5].

As mentioned previously, two types of samples were prepared for the experimental analysis. In the first type of sample, the fiber was coated with a thin layer of EPON Resin 871 (aliphatic polyepoxide). This resin is an amber, low viscosity liquid which imparts increased flexibility to EPON 828 compositions. It is known to lower the modulus and glass transition temperature of the cured epoxy. Figure 3 is a plot of glass transition temperature determined by differential scanning calorimetry (DSC) as a function of percent EPON 871 by weight added to the EPON 828/PACM resin system. At concentrations greater than 45 percent, the T_g of the epoxy falls below 60°C. For the second type of sample, fibers were left untreated.

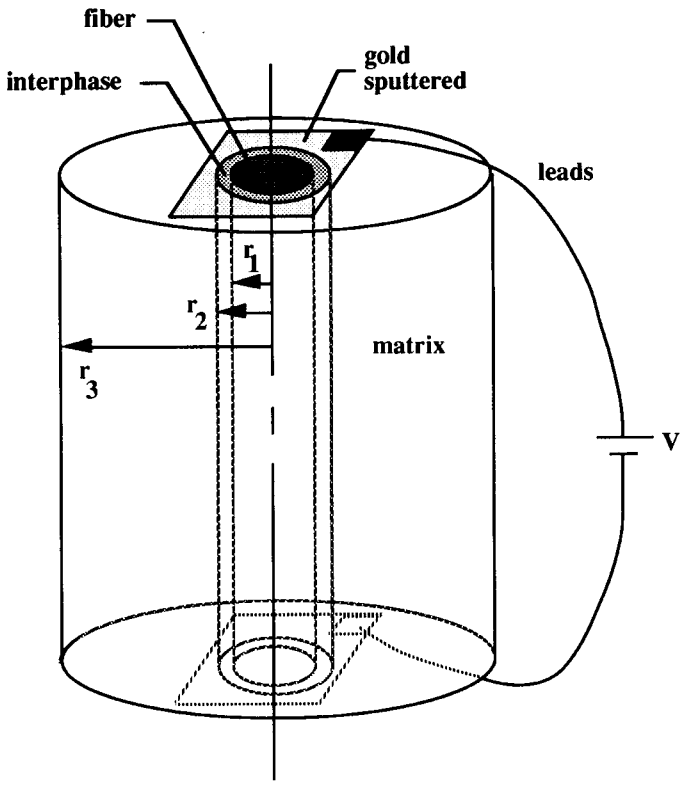

Figure 2: Schematic of single fiber sample for micro-interferometric studies.

Table 1: Fiber and Matrix Material Properties

Property	30 μm Carbon Fiber	EPON 828/PACM
E (GPa)	41.0	2.45
α (x10^{-6} $^{\circ}C^{-1}$)	-0.5	54.0
K ($\frac{W}{m\,^{\circ}C}$)	8.3	0.18
ν	0.22	0.33

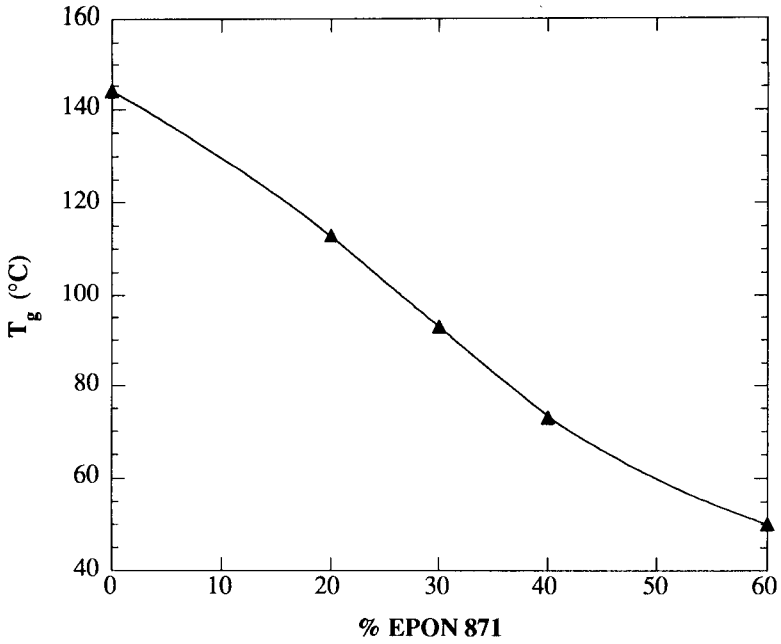

Figure 3: Glass transition temperature of the EPON 828/EPON871/PACM mixture as a function of percent EPON 871 by weight.

Samples were then prepared by placing the single fiber, coated or uncoated, into the center of a mold which was then filled with a stoichiometric mix of resin (28 parts PACM 20 to 100 parts EPON 828). All samples were held for 1 hour at $80°C$ to minimize the bubbles in the resin phase, then cured for 1 hour at $150°C$, and allowed to slow cool to room temperature overnight. Specimens were cut to a length of approximately 2 cm and the front and back faces were polished metallographically. Polishing of the front face on which the measurements were made was critical to insure a specularly reflective surface. The radius of the fiber was determined to be 17.2 μm from a photomicrograph of the sample surface. The outer radius of the samples measured 15.88 mm.

To heat a sample, a small current of 10.0 mA was passed through the fiber, as leads were attached to both the front and back polished faces of the specimen. A thin layer of gold was sputtered onto the surface to provide both a current conduction path and a highly reflective surface across the circular cross-section of the fiber/matrix interface. There were several advantages to heating the sample electrically in this manner. A repeatable, radial temperature field was generated in the sample which could be predicted analytically. The equilibrium time for heating and cooling the region of interest was small (typically less than ten seconds). Finally, there was minimal convection of heat

into the interferometer path minimizing thermal effects on the apparatus.

Analytical prediction of the temperature distribution in the sample required the solution of the heat conduction equation for an electrically heated fiber embedded in an epoxy matrix. This problem has been solved previously by Sottos, et al. [13] and was used to calculate the the steady state temperature field. As a result of applying 58 mW of power to the samples, the temperature in the fiber was predicted to be nearly constant at $60°C$, while the matrix temperature was found to decrease rapidly away from the interface. The analytical prediction for fiber temperature was compared with experimental values and found to differ by less than five percent [13].

3.2 Results

To measure the thermal displacements in the interphase, it was convenient to make measurements on single scan lines extending across the fiber center. The magnification of the interferometer was 25X for these measurements so that the far field matrix could be included in the scan. Heating the sample caused the matrix to expand upwardly and pull the fiber with it. Subtraction of an initial unheated scan line from the heated scan line yielded the net thermal displacement of the region.

A series of displacement measurements was made on both types of samples. All of the displacement data were normalized to account for small differences in sample hieght and to facilitate theoretical comparisons. Figure 4 is a plot of the thermal displacements for both the coated and uncoated single fiber samples. The displacements are plotted as a function of radial distance with the fiber center at $r = 0$. The displacement data was averaged for three consecutive runs on each sample and then normalized by subtracting from each point the value of the displacement of a reference point at 20 fiber radii out. The displacement of the fiber is nearly constant. However, there is a sharp rise in the displacement of the matrix near the interface, which peaks at about 5 fiber radii out. After this point, the matrix displacements decrease almost linearly with radial distance. The gradient at the interface and consequently the displacement of the fiber are significantly larger, however, for the coated fiber. Hence, the interferometric method was capable of detecting different surface treatments or coatings applied to the fiber.

3.3 Comparison of Experiment and Theory

In a previous study [16], a thermal displacement solution was derived for a three phase, finite, composite cylinder model using a displacement potential approach. The indices $i = 1, 2, 3$ were used to denote the fiber, interphase and matrix domains, respectively. The interphase, $r_1 < r < r_2$, was treated as a region with uniform material properties, different from those of the matrix or the fiber. The width of the interphase, $r_2 - r_1$, was denoted as λ. The matrix, fiber and interphase were assumed to be isotropic. This assumption was a major one since the carbon fiber was actually transversely isotropic. Because the out-of-plane thermal displacements are dominated by the axial properties,

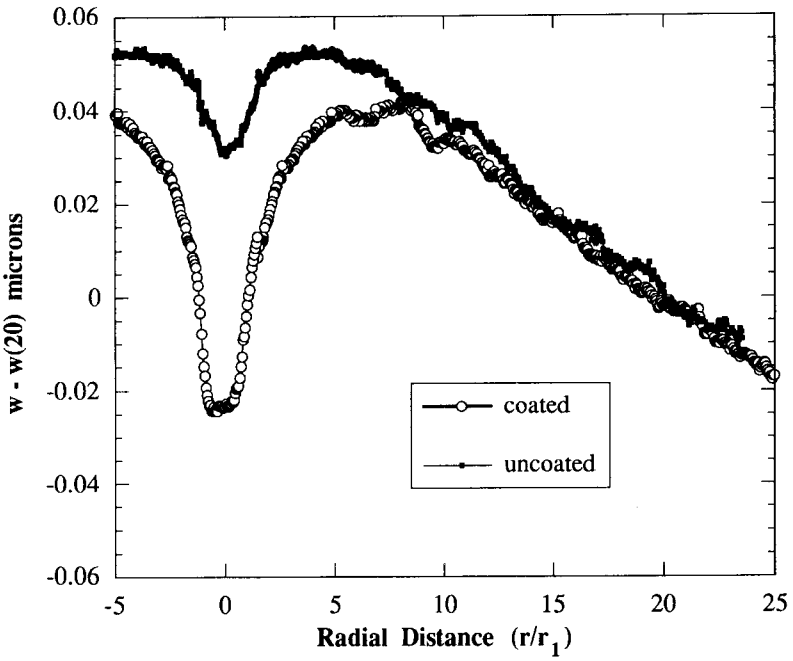

Figure 4: Average axial thermal displacement as a function of radial distance from the fiber center for the coated and uncoated single fiber samples.

the fiber properties chosen in table 1 were the axial values. Solution of the governing equations yielded the following expression for axial displacement [16]:

$$w^{(i)} = \sum_{n=1}^{\infty} [\, -\frac{1}{2} m^{(i)} r \, f_{1n} + D_{1n}^{(i)} \, h_{3n}^{(i)} + D_{2n}^{(i)} \, g_{3n}^{(i)} + D_{3n}^{(i)} \, h_{4n}^{(i)} + D_{4n}^{(i)} \, g_{4n}^{(i)} \,] \sin(\kappa_n z) \qquad (1)$$

The functions, $h_{3n}^{(i)}, h_{4n}^{(i)}, g_{3n}^{(i)}, g_{4n}^{(i)}$ and f_{1n}, are combinations of modified Bessel functions and can be expressed in terms of the engineering constants, E and ν, as follows:

$$f_{1n} = [A_n I_1(\kappa_n r) - B_n K_1(\kappa_n r)] \qquad (2)$$

$$h_{3n}^{(i)} = \left(\frac{1 + \nu^{(i)}}{E^{(i)}} \right) \kappa_n^2 \, I_0(\kappa_n r) \qquad (3)$$

$$h_{4n}^{(i)} = \left(\frac{1 + \nu^{(i)}}{E^{(i)}} \right) \kappa_n^2 \, [4(1 - \nu) \, I_0(\kappa_n r) + \kappa_n \, r \, I_1(\kappa_n r)] \qquad (4)$$

$$g_{3n}^{(i)} = \left(\frac{1 + \nu^{(i)}}{E^{(i)}} \right) \kappa_n^2 \, K_0(\kappa_n r) \qquad (5)$$

$$g_{4n}^{(i)} = \left(\frac{1 + \nu^{(i)}}{E^{(i)}} \right) \kappa_n^2 \, [-4(1 - \nu) \, K_0(\kappa_n r) + \kappa_n \, r \, K_1(\kappa_n r)] \qquad (6)$$

The twelve constants, $D_{1n}^{(i)}$, $D_{2n}^{(i)}$, $D_{3n}^{(i)}$, and $D_{4n}^{(i)}$, were determined by systematic application of the boundary conditions on the cylinder.

Through the use of equation (1), the theoretical displacements were calculated and compared with the experimental results. The necessary fiber and matrix properties are listed in table 1. For a first comparison, the influence of an interphase was not considered. The properties of the region, $r_1 < r \leq r_2$, were chosen to be identical to those of the surrounding matrix. In figure 5, the resulting theoretical displacement curve is plotted along with the experimental profiles as a function of radial distance from the fiber center at $r = 0$. The displacement values have again been normalized by subtracting the value of the displacement at 20 fiber radii out from the fiber.

For the uncoated fiber case, the theoretical and experimental predictions were in excellent agreement from about 5 fiber radii out to the far field matrix. At closer than 5 fiber radii to the fiber center, the two curves started to differ dramatically. The experimental value for the fiber displacement was much less than predicted by theory for a uniform matrix with no interphase. Consequently, there was a much sharper gradient in the experimental displacement curve at the fiber/matrix interface. This result was consistent with the measurements made in previous studies [16]. When the sample was heated, the matrix material near the fiber surface did not behave as predicted for a uniform matrix with no interphase, while the matrix in the far field did behave as the neat resin.

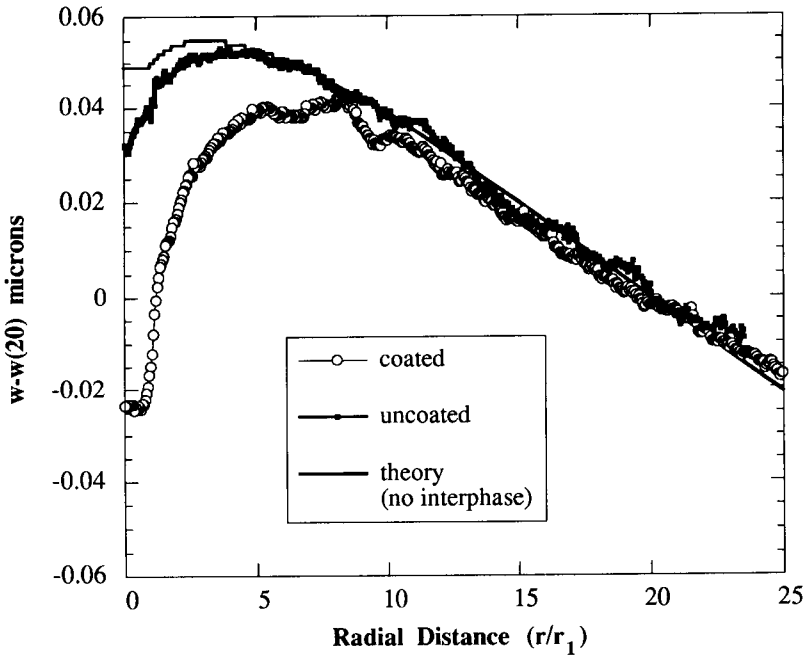

Figure 5: Comparison of theoretical and experimental displacements for uncoated and coated fiber samples with no interphase.

For the coated fiber the difference between the theoretical prediction and the experimental profile was more dramatic. As discussed previously, the gradient in displacement near the fiber/matrix interface was significantly larger. Theory and experiment were only in agreement at greater than 10 fiber radii from the fiber center. Hence, the effects of the coating propagated out into the matrix further than the thickness of the coating itself.

In the next step of the analysis, the experimental profiles for both types of samples were compared to displacement predictions for a distinct interphase region with properties significantly different from the neat matrix. Three unknown variables, the interphase width, elastic modulus and coefficient of thermal expansion, were necessary to predict the thermal displacement field. The thermal conductivity and Poisson's ratio of the interphase were assumed to have the same value as the matrix. The value of the interphase modulus required to most closely model the experimental profiles was highly dependent on the chosen interphase width. As the width of the interphase region, λ, was made smaller, a lower value of interphase modulus was needed to model the sharp displacement gradients observed experimentally. For larger interphase widths, the interphase modulus did not have to be quite as low to produce the necessary gradient.

Table 2: EPON 828/PACM Material Properties above T_g

E (GPa)	0.045
α (x10^{-6} $^{\circ}C^{-1}$)	160.0

However, if the interphase width was chosen too large, the far field displacements would no longer correspond with the experimental profiles.

In previous interferometric studies it was shown for thin interphase regions ($\lambda \leq 0.5$ fiber radii), a modulus an order of magnitude lower than that of the neat resin, most closely matched the experimental data [16]. To obtain a modulus this low, the epoxy would have to be heated to a temperature above its glass transition, T_g. Polymers typically experience an order of magnitude drop in modulus accompanied by a two or three fold increase of the coefficient of thermal expansion at temperatures above their T_g. Palmese [5] has measured the value of the modulus and coefficient of thermal expansion above T_g for the EPON 828/PACM system. These values are listed in table 2.

If the interphase parameters are assigned the values in table 2, a value of $\lambda = 0.08$ fiber radii as the interphase width most closely matches the experimental data for the uncoated fiber sample. Figure 6 compares the uncoated experimental observations with the theoretical displacement predictions for an interphase characterized by the properties in table 2. The properties of the matrix are assigned those of the neat resin given in table 1. Due to the size of the photodetector window, an averaging effect occurs when there are sharp gradients in the experimental data. The window is 0.75 mm in diameter, which translates into 1.4 fiber radii on the magnified image plane. Thus, any sharp change in profile will be averaged across the window. Ideally, the experimental data should be deconvoluted to eliminate the effects of the circular detector window. It is much more convenient, however, to perform a running average of the theoretical displacement predictions. Consequently, the theoretical predictions in figure 6 have been averaged over the diameter of the detector window. There is a small discrepancy between the two curves, but this may attributed to the limitations of the theoretical displacement model.

For the coated fiber, a much larger interphase width of $\lambda = 0.6$ fiber radii is necessary to match the sharp displacement gradients near the fiber/matrix interface. The averaged theoretical predictions are plotted with the experimental profile for the coated fiber in figure 7. In this case, an even larger discrepancy between theory and experiment exists at a radial distance between 2 and 10 fiber radii. In the theoretical model, a uniform interphase region with no property gradients was considered. It is likely that material properties across such a large interphase region will vary smoothly back to the values of the bulk matrix. Ideally, a more sophisticated computational model of the thermal displacements could be developed to more accurately match the properties of the interphase. The current model, however, is sufficient to show the trends in the interphase properties needed to produce the measured displacement profiles.

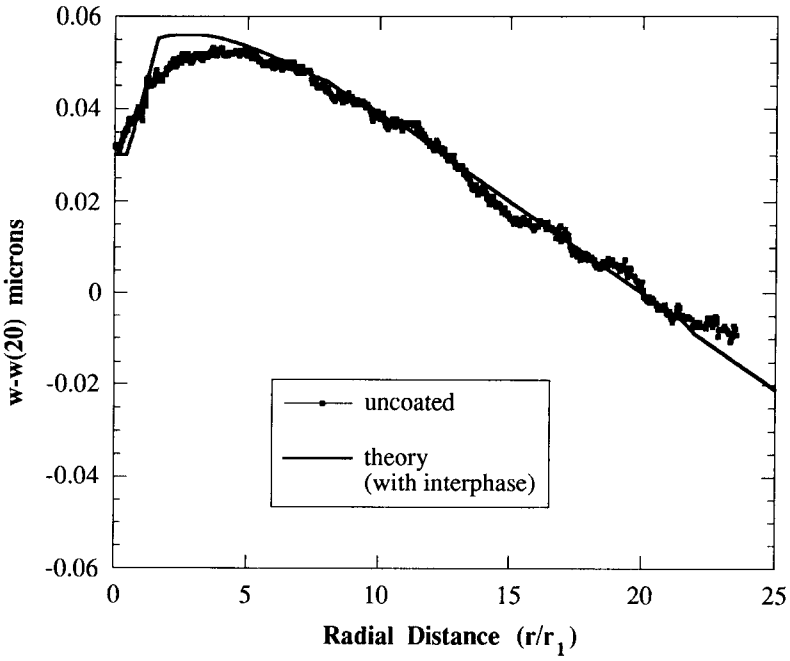

Figure 6: Comparison of theoretical and experimental displacements for uncoated fiber with interphase.

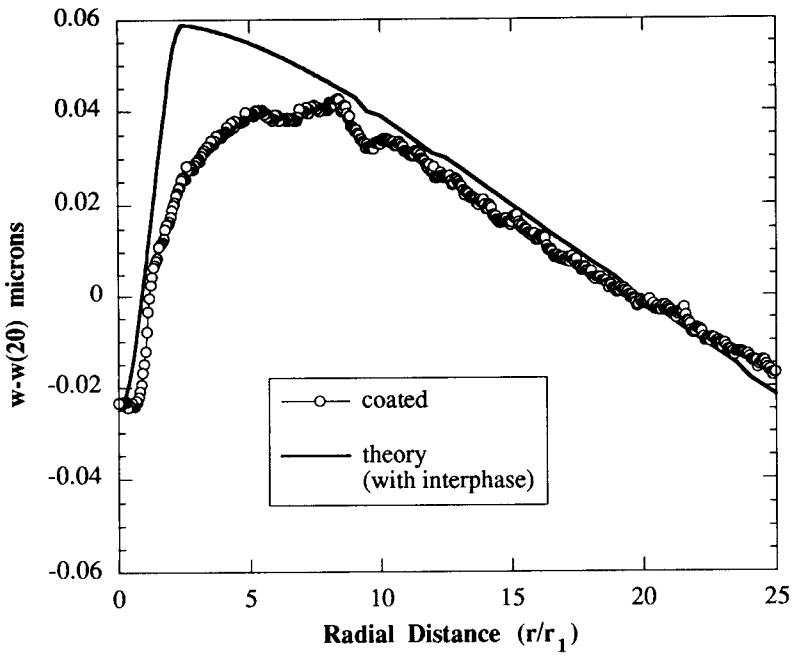

Figure 7: Comparison of theoretical and experimental displacements for coated fiber with interphase.

The interface is the physical boundary between fiber and matrix that serves as the region where stresses acting on the matrix are transferred to the fibers. It is essential to have some measure of the interfacial bond strength for the evaluation of composite properties and the development of well designed interfaces. A number of methods for measuring the stress state and the strength of the bond at the interface have appeared in the literature.

The single fiber critical length method was originally developed by Kelly and Tyson [17] for metals. This method has been adopted by Fraser, et al. [18], Drzal [19] and many others for determining the interfacial shear strength in polymer composites. In the current study, single fiber critical length tests were performed for the two different interphase conditions over a range of temperatures. From the results, the influence of the interphase glass transition temperature on the interfacial shear strength could be assessed. The interfacial shear strength was expected to significantly decrease if the T_g of the interphase was exceeded. As for the micro-interferometric results, the behavior observed for untreated fibers should be enhanced by coating the fibers with a low T_g resin.

4.1 Sample Preparation and Procedure

Single fiber critical length tests were performed on specimens consisting of a 7μm Hercules AS4 carbon fiber embedded in the EPON 828/PACM epoxy matrix. As for the interferometric experiments, two types of samples were prepared. In the first type of sample, AS4 fibers were coated with a thin layer of EPON 871 resin to reduce the glass transition of the interphase. For the second type of sample, fibers were left untreated. The single fibers were then embedded in dogbone coupons of the matrix as described by Drzal, et al. [20]. The single fiber dogbone specimens were then cured exactly as described for the interferometric samples.

Once fabricated, the samples are loaded in tension using a small hand operated tensile apparatus so that the fiber fractures into small pieces within the matrix. The fracture process continues until the fiber pieces reach a minimum critical length. Upon further extension, the fiber will not continue to break into smaller lengths. The fiber lengths as well as the fiber diameter are then carefully measured under the microscope. In theory, the interfacial shear strength is inversely proportional to the critical length and is expressed as follows

$$\tau = \frac{\sigma_f d}{2l_c} \tag{7}$$

where l_c is the critical length, d is the fiber diameter, and σ_f is the fiber strength. However, if many samples are tested the data can be fitted to a two parameter Weibull distribution. The mean interfacial shear is calculated by the relation [20]

$$\tau = \frac{\sigma_f}{2\beta}\Gamma\left(1 - \frac{1}{\alpha}\right) \tag{8}$$

The parameters α and β are solutions to

$$\beta = \left(\frac{1}{n}\Sigma X_i^{\alpha}\right)^{\frac{1}{\alpha}} \tag{9}$$

$$\frac{\Sigma X_i^{\alpha}}{ln(\Sigma X_i)}\Sigma X_i^{\alpha} - \frac{1}{\alpha} - \frac{ln(\Sigma X_i)}{n} = 0 \tag{10}$$

where $X_i = \frac{l_c}{d}$, n is the number of measurements, and Γ is the gamma function. Both types of samples were tested at room temperature, $60°C$, $80°C$, and $100°C$. Heated tests were performed in a temperature controlled oven normally used for full scale mechanical testing and then examined under the microscope. Fifteen samples were tested at each temperature.

4.2 Results and Discussion

The results of the single fiber critical length tests are summarized in Figure 8. Interfacial shear strength is plotted as a function of temperature for both the coated and uncoated samples. Note that all values of interfacial shear strength have been normalized by the value at room temperature. For the uncoated samples, there was a distinct decrease in interfacial shear strength with temperature. Heating to a moderate temperature of $60°C$ caused a ten percent reduction in the average shear strength. Heating to $100°C$ caused nearly a 25 percent reduction in shear strength. The observed reduction in shear strength at both $60°C$ and $80°C$ was enhanced for the coated fiber samples, as there was a seventeen and twenty three percent reduction in shear strength, respectively. However, at $100°C$ there was very little difference between the interfacial shear strength values for both types of samples.

The observed decrease in interfacial shear strength with temperature is consistent with the results of a previous study by Ohsawa, et al. [21]. In this work, the critical length of the a glass fiber/epoxy resin system was found to significantly increase with temperature, causing a corresponding decrease in interfacial shear strength. The authors concluded that the decreasing values could not be explained solely by thermal stresses between the fiber and matrix and suggested that this phenomenon was brought about by a decrease in the shear strength of the matrix. The Ohsawa tests were performed in a range from $40°C$ - $100°C$, while the glass transition temperature of the epoxy matrix was approximately $60°C$. Hence, it was reasonable to expect a large decrease in interfacial shear strength in their chosen temperature range.

In the current study, however, the glass transition temperature of the neat resin was approximately $160°C$. This value was considerably higher than the experimental temperature range. For both interphase conditions investigated, a reduction in interfacial shear strength occurred at moderate temperatures, far from the T_g of the bulk resin). Additionally, the reduction in shear strength was enhanced by the presence of the low T_g coating. Hence, the results of the single fiber critical length tests also supported the existence of a reduced glass transition temperature at the fiber surface.

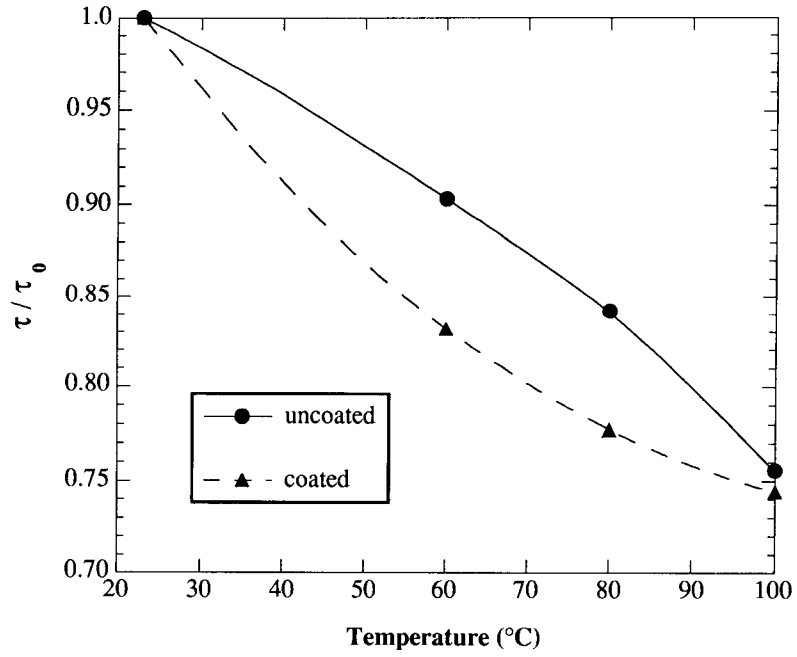

Figure 8: Interfacial shear strength (normalized by the room temperature value) as a function of temperature for the coated and uncoated samples.

5. CONCLUSIONS

Both the interferometric measurements and the single fiber critical length tests supported the existence of a lower glass transition temperature near the fiber/matrix interface. A comparison of the interferometric profiles measured for both types of samples with theoretical displacement predictions indicated that the value of the matrix properties near the fiber surface differed appreciably from the value in the neat resin. For the uncoated fiber, a thin interphase region of approximately 0.08 fiber radii, with a modulus an order of magnitude lower than the neat resin, most closely matched the experimental data. For the coated fiber, a larger interphase region of approximately 0.6 fiber radii is predicted for the measured displacement profiles. In order for the modulus to have such a low value (in both samples), the epoxy in the interphase would have to be heated to a temperature above its glass transition. The enhancement of the displacement gradient for the fiber coated with a low T_g resin provides further evidence for this phenomenon. Additionally, the results of the single fiber critical length tests for both interphase conditions investigated showed a pronounced reduction in interfacial shear strength at moderate temperatures, far from the T_g of the bulk resin. The reduction in shear strength was also enhanced by the presence of the low T_g coating.

The existence of a depressed glass transition temperature in the interphase is consistent with the findings of several other researchers [2,5,6,7,8] as discussed in Section 2. An interphase region with a low T_g will have a pronounced effect on the performance of a composite. In the current study it has been shown that the interphase can be tailored to enhance this behavior. Consequently, work is in progress to further investigate interphases with a higher glass transition temperature which could hinder this effect.

6. ACKNOWLEDGEMENTS

This work was supported by the Office of Naval Research. The technical support and guidance of W.R. Scott at the Naval Air Warfare Center (NAWC), Warminster, PA as well as the use of the facilities at NAWC are greatly appreciated.

7. REFERENCES

[1] P.W. Erickson, A. Volpe, and E.R. Cooper. Chemical and physical effects of glass surfaces upon laminating resins. In *Proceedings of the* 19^{th} *Conference SPI*, 1966. Section 21-A.

[2] Y.S. Lipatov, V.F. Babich, and V.F. Rosovizky. Effect of filler on the relaxation time spectra of filled polymers. *Journal of Applied Polymer Science*, 20:1787–1794, 1976.

[3] G.C. Papanicolaou and P.S. Theocaris. Thermal properties and volume fraction of the boundary interphase in metal-filled epoxies. *Colloid and Polymer Science*, 257:239–246, 1979.

[4] A. Garton and J.H. Daly. Characterization of the aramid: Epoxy and interphases. *Polymer Composites*, 6(4):195–199, 1985.

[5] G.R. Palmese. *The Interphase in Thermosetting Composites.* PhD thesis, Department of Chemical Engineering, University of Delaware, Newark, Delaware 19716, 1991.

[6] G.A. Pogany. The β-relaxation in epoxy resins, the temperature and time-dependence of cure. *Journal of Materials Science*, 4:405–409, 1969.

[7] R.J. Crowson and R.G.C. Arridge. The elastic properties in bulk and shear of a glass bead-reinforced epoxy resin composite. *Journal of Materials Science*, 12:2154–2164, 1977.

[8] G.C. Papaniclaou, S.A. Paipetis, and P.S. Theocaris. The concept of boundary interphase in composite mechanics. *Colloid and Polymer Science*, 256:625–630, 1978.

[9] N.R. Sottos, W.R. Scott, and M.J. Ryan. Repeatability of local thermal displacement measurements near the fiber/matrix interface using micro-interferometry. In *Review of Progress in Quantitative Nondestructive Evaluation*, volume 10A. Plenum Press, New York, 1990.

[10] W.R. Scott, S. Huber, and M. Ryan. An image scanning heterodyne microinterferometer. In *Review of Progress in Quantitative Nondestructive Evaluation*, volume 7B, pages 1065–1073. Plenum Press, New York, 1988.

[11] W.R. Scott, M.J. Ryan, D.M. Granata, and N.R. Sottos. Nondestructive evaluation and characterization of composite materials microinterferometry. In *1st Navy Independent Research/Independent Exploratory Development Symposium*, volume 1, pages 481–491, 1988. CPIA Publication 492.

[12] S. Huber, W.R. Scott, and R. Sands. Detection and analysis of waves propagating in boron/aluminum composite materials. In *Review of Progress in Quantitative Nondestructive Evaluation*, volume 6B, pages 1065–1073. Plenum Press, New York, 1987.

[13] N.R. Sottos, W.R. Scott, and R.L. McCullough. Micro-interferometry for measurement of thermal displacements at fiber/matrix interfaces. *Experimental Mechanics*, 31(2), 1991.

[14] M.J. Ryan, W.R. Scott, and N.R. Sottos. Scanning heterodyne micro-interferometry for high resolution contour mapping. In *Review of Progress in Quantitative Nondestructive Evaluation*, volume 10A. Plenum Press, New York, 1990.

[15] C.C. Chamis. Mechanics of load transfer at the interface. In E.P. Pluddemann, editor, *Composite Materials*, volume 6, pages 32–77. Academic Press, New York, 1974.

[16] N.R. Sottos, R.L. McCullough, and W.R. Scott. The influence of interphase regions on local thermal displacements in composites. *Composites Science and Technology*, 1991. In Press.

[17] A. Kelly and W.R. Tyson. Tensile properties of fibre-reinforced metals: copper/tungsten and copper/molybdenumm. *Journal of Mechanics and Physics of Solids*, 13:329–3, 1965.

[18] W.A. Fraser, F.H. Achker, and A.T. DiBenedetto. A computer modeled single filament technique for measuring coupling and sizing agent effects in fiber reinforced composites. In *Proceedings of 30th Annual Technical Conference of the Society of Plastics Engineers*, pages 22–A, 1975.

[19] L.T. Drzal. Composite interphase characterization. *SAMPE Journal*, Sept./Oct.:7–13, 1983.

[20] L.T. Drzal, M.J. Rich, J.D. Camping, and W.J. Park. Interfacial shear strength and failure mechanisms in graphite fiber composites. In *Proceedings of the 35th Annual Technical Conference of the Reinforced Plastics/Composites Institute*, pages 20–C. The Society of the Plastics Industry, Inc., 1980.

[21] T. Ohsawa, A. Nakayama, M. Miwa, and A. Hawegawa. Temperature dependence of critical fiber length for glass fiber-reinforced thermosetting resins. *Journal of Applied Polymer Science*, 22:3203–3212, 1978.